Jurnal Polimesin
Department of Mechanical Engineering
State Polytechnic of Lhokseumawe
http://e-jurnal.pnl.ac.id/polimesin
e-ISSN : 2549-1999 No. : 4 Month : August
p-ISSN : 1693-5462 Volume : 21 Year : 2023

Article Processing Dates: Received on 2023-03-29, Reviewed on 2023-06-19, Revised on 2023-07-04, Accepted on 2023-07-07 and Available online on 2023-08-25

CFD Simulation of oxy-fuel combustion using turbulent non-premixed combustion with medium-rank coal from Kalimantan Indonesia

A. P. Nuryadi*[1], R. J. Komara[1], M. P. Helios[1], I. Wulandari[2], Chairunnisa[1], Fitrianto[1]

[1]Research Center for Energy Conversion and Conservation, National Research and Innovation Agency, South Tangerang, 15314, Indonesia

[2]Research Center for Hydrodynamics Technology, National Research and Innovation Agency, Surabaya, 60112, Indonesia

*Corresponding author: agus130@brin.go.id

Abstract

Carbon capture technology connected with oxy-fuel combustion has a high potential for reducing CO_2 emissions, particularly in coal-fired power plants. However, the distinct characteristics of each coal depend on its origin. This study analyzes coal combustion from Kalimantan using a drop tube furnace and varying the volume of oxygen: coal (21 vol.% O_2), OF25 (coal with 25 vol.% O_2), OF30 (coal with 30 vol.% O_2), the non-premixed combustion model and a structured grid. Probability Density Function (PDF) models were used for combustion chemistry. The overall combustion temperature distribution and the amounts of O_2, H_2O, C, and CO_2 in combustion products were visualized. The numerical results show that increasing the volume of oxygen leads to an increase in temperature distribution for OF25 and OF30, but the flame is shorter than for coal. During combustion, the mass fraction of oxygen remains in the furnace and H_2O increases. Carbon burns quickly and is depleted, whereas the CO_2 content increases along with the volume of oxygen, making the CO_2 capture process easier. The results obtained from the numerical analysis can offer valuable insights for enhancing the design of combustion chambers in oxy-fuel boilers for better modeling of pulverized coal especially using Kalimantan coal.

Keywords:

Non-premixed, oxy-fuel combustion, probability density function, Kalimantan coals.

1 Introduction

Recently, the impact on the environment and public health due to the release of Greenhouse Gases (GHG) by electricity production has been recognized as a significant contributor to global climate change [1]. Carbon dioxide emissions are the most important contributor to greenhouse gas emissions in the atmosphere. Fossil fuels satisfy about 85% of the world's electricity demand [2]. Various carbon capture methods have been created to maintain the continuous functioning of conventional combustion machinery while reducing environmental impact, encompassing pre-combustion capture, post-combustion capture, and oxy-fuel combustion [3] [4]. Oxy-fuel combustion is considered one of the most effective technologies for controlling and reducing emissions of pollutants from Pulverized Coal (PC) boilers in compliance with new environmental and political regulations designed to combat global warming [5] [6]. The flue gas mainly comprises CO_2 and H_2O when N_2 is removed from the combustion medium. A condensation process is used on the flue gas to obtain nearly pure CO_2. After that, the pure CO_2 can be extracted and used for commercial purposes, such as enhanced oil recovery, by injecting it into depleted oil and gas reservoirs [7]. Increasing oxygen fraction, the flame temperature will rise and becomes more confined to the burner exit plane due to higher oxygen consumption [8]. Studies have shown that increased CO_2 concentrations positively affect devolatilization but have no impact on subsequent char combustion. However, some studies indicate that oxy-fuel does not directly influence devolatilization but affects char reactions depending on the coal type. To achieve similar or better burnout than in air [9], the oxygen concentration in O_2/CO_2 conditions must exceed 21%, and low recycled flue gas rates can improve burnout in oxy-fuel conditions [8]. Numerical simulations are used to develop models to facilitate reliable predictions for these processes.

Using Computational Fluid Dynamics (CFD) to assess oxy-fuel combustion is an important subject, and studies often examine hypothetical oxy-coal combustion in conventional boilers. Following is a literature study using ANSYS using global mechanism combustion. The use of the CFD model with FG-DVC coal devolatilization kinetics in an Entrained Flow Reactor (EFR) for oxy-coal combustion resulted in significantly better agreement with experimental values compared to the predictions obtained using the default kinetics of the ANSYS Fluent program [10]. The study aimed to validate experimental observations in a lab-scale Drop-Tube Furnace (DTF) by utilizing ANSYS Fluent to numerically model the combustion of air-dried Victorian brown coal in O_2/N_2 and O_2/CO_2 mixtures containing 21%-30% O_2. Additionally, a refined two-step mechanism was employed to simulate the volatile oxidation during the oxy-firing of methane [11]. The study examined the use of oxy-fuel combustion with Victorian brown coal in a 3 MWth pilot-scale facility. Two coal samples, one wet and the other air-dried, were tested under different firing modes (air and oxy) with varying levels of oxygen ranging from 27% to 40% in the furnace, and the experimental data were analyzed using Fluent 13 designed for oxy-fuel combustion [12]. The ANSYS Fluent was employed to retrofit existing boilers with oxy-fuel combustion, utilizing a global mechanism combustion approach. The enhanced burner design demonstrated greater versatility, ensuring consistent ignition and combustion in conventional air-based and oxy-fuel conditions with an oxygen mixture [13]. Using ANSYS, the estimation of oxy-coal combustion in a cement rotary kiln was conducted by varying the O_2 volume ratios within the range of 21% to 31%. The findings indicated a notable rise in temperature within the rotary kiln, with coal particles exhibiting faster combustion near the burner, resulting in an augmented degree of burnout. This simultaneous increase in burnout degree corresponds to enhanced combustion efficiency, reducing fuel consumption [14]. A numerical analysis examined how varying oxygen levels in a drop tube furnace impact its performance. When comparing the same oxygen concentration, the particle and burning temperatures were significantly lower in the case of oxygen, and the combustion of volatiles and char was delayed compared to the point with air [15]. However, a global mechanism combustion study needs detailed chemical combustion reactions and high computation.

The Probability Density Function (PDF) model is reasonably practical and accurate because it directs translating species transport equations [16] [17]. A numerical study with the plasma system was created using the PDF model to simulate the flow inside a vent during coal combustion and ignition [18]. The pulverized coal of NOx reduction in combustion by creating a PDF model was utilized and employed a computational model [19]–[23]. Several gases were used to demonstrate how the dilution of the oxidizer is consistent with those obtained through

experimentation [24]. The study integrates the flamelet produced by non-premixed gaseous flames with the equation for transporting mixture fraction variance, utilizing a considered PDF method to model the exchange between turbulence and chemistry [24]. A simulation study of pulverized coal in a corner-fired furnace used the non-premixed with Mixture Fraction Probability Density Function (MF-PDF) combustion to reveal NO reduction in fuel-rich conditions and comparison between atmospheric conditions and low temperatures [25]. Based on those studies, oxy-fuel combustion could be investigated using non-premixed combustion with the PDF model.

A DTF experiment was conducted to investigate the combustion properties of coal under conditions similar to those found in supercritical or subcritical coal-fired power plant boilers. The experiment was set up with specific operational factors taken into account, such as furnace temperature, coal particle size, coal feed rate, and water. The DTF was operated at 1200 ºC, a standard temperature for coal-fired power plants. The study examined several combustion parameters, such as ignition time, ignition temperature, burnout time, and combustion temperature [26]–[29]. This study investigated the combustion of coal from Kalimantan [30] in a Drop Tube Furnace (DTF) while varying the volume of oxygen, specifically coal (21 vol.% O_2), OF25 (25 vol.% O_2) and OF30 (30 vol.% O_2), using the non-premixed combustion model. The Probability Density Function (PDF) was used to depict turbulence and combustion chemistry. The primary objective of this research is to assess how varying levels of oxygen impact combustion using the ANSYS Fluent.

2 Mathematical Models

The governing equations are [30]–[32]:

1) Continuity equation (Eq. 1)

$$\frac{\partial \rho}{\partial t} + \nabla.(\rho\,\vec{u}) = 0 \tag{1}$$

2) Momentum equation (Eq. 2)

$$\frac{\partial}{\partial t}(\rho\vec{u}) + \nabla.(\rho\vec{u}\vec{u}) = -\nabla \mathrm{p} + \nabla.(\bar{\bar{\tau}}) + \rho\vec{g} \tag{2}$$

3) The energy equation for the non-premixed combustion model (Eq. 3)

$$\frac{\partial}{\partial t}(\rho H) + \nabla.(\rho\vec{u}H) = \nabla.\left(\frac{k_t}{C_p}\nabla \mathrm{H}\right) + S_h \tag{3}$$

4) H is the total enthalpy (Eq. 4)

$$H = \sum_j Y_j H_j \tag{4}$$

S_h in Eq. 3 is the source of energy due to chemical reaction (Eq. 5)

$$S_h = -\Sigma\frac{h_j^0}{M_j}R_j \tag{5}$$

5) The equation used to transport turbulent kinetic energy (K) and turbulent effects were considered by utilizing the k-epsilon turbulent model [30] (Eq. 6)

$$\frac{\partial(\rho k)}{\partial t} + \nabla.(\rho\vec{u}k) = \nabla.\left[\left(\mu + \frac{\mu_t}{\sigma_k}\right)\nabla k\right] + G_k - \rho\varepsilon + P_K \tag{6}$$

6) The Discrete Ordinates (DO) model [33] (Eq. 7)

$$\nabla.(I_\lambda(\vec{r},\vec{s})\vec{s}) + (a_\lambda + \sigma_s)I_\lambda(\vec{r},\vec{s}) = a_\lambda n^2 I_{b\lambda} + \frac{\sigma_s}{4\pi}\int_0^{4\pi} I_\lambda(\vec{r},\vec{s}')\varphi(\vec{s},\vec{s}')d\Omega' \tag{7}$$

7) Discrete Phase Model (DPM) trajectory coal (Eq. 8)

$$m_p\frac{d\vec{v}_p}{dt} = \Sigma\vec{F} \tag{8}$$

$\vec{F}$ is an external force. The dominant forces that affect the particle are drag and buoyancy forces. This leads to a specific equation of motion [34] (Eq. 9)

$$\frac{d\vec{v}_p}{dt} = F_D\left(\vec{v} - \vec{v}_p\right) + \frac{g(\rho_p - \rho)}{\rho_g} \tag{9}$$

8) In this equation, Re_p is the particle Reynolds number, which is given as [34] (Eq. 10)

$$Re_p = \left(\frac{\rho d_p|\vec{v}_p - \vec{v}|}{\mu}\right) \tag{10}$$

9) The CD is the Drag coefficient, as a function of particle Reynolds number is defined [34] (Eq. 11)

$$C_D = \frac{24}{Re}(1 + 11.2355Re^{0.653}) + \frac{(-0.8271)Re}{8.8798 + Re} \tag{11}$$

10) Coal devolatilization [30] (Eq. 12)

$$\frac{-dm_p}{dt} = k(m_p - \left(1 - f_{v,0} - f_{w,0}\right)m_{p,0}) \tag{12}$$

where: $K = A_1 exp^{\frac{-\varepsilon}{RT}}$

11) The Mixture Fraction and PDF Modeling [30]:
Mean mixture fraction $\bar{f}$ (Eq. 13)

$$\frac{\partial(\rho\bar{f})}{\partial t} + \nabla.\left(\rho\bar{f}\vec{u}\right) = \nabla.\left(\frac{\mu_t}{\sigma_t}\nabla\bar{f}\right) + \frac{\dot{m}_{p,0}}{m_{p,0}}(m_{p,in} - m_{p,out}) \tag{13}$$

Mean mixture fraction variance $\bar{f}'^2$ (Eq. 14)

$$\frac{\partial(\rho\bar{f}'^2)}{\partial t} + \nabla.\left(\rho\bar{f}'^2\vec{u}\right) = \nabla.\left(\frac{\mu_t}{\sigma_g}\nabla\bar{f}'^2\right) + 2.86\mu_t\left(\nabla\bar{f}'^2\right) - 2\rho\frac{\varepsilon}{k}\bar{f}'^2 \tag{14}$$

Table 1 contains the values from the proximate and ultimate analysis of Kalimantan coal and combustion products to determine the species selection to be included in the analysis.

3 Numerical Procedure

This study is 2D symmetry geometry based on a Drop Tube Furnace (DTF). The wall of DTF is an alumina ceramic tube with a total height of 1200 mm and a radius is 35 mm with a temperature of 1200 ºC. The condition is adopted to simulate a pulverized coal boiler [35]. Fluent Software is employed in the simulation to resolve the partial differential equations regulating multiple species' flows. A control volume is used, where each node corresponds to the computational domain so that the partial differential equations are integrated into each limited volume [36]. All convective terms use the QUICK scheme, and for velocity, the SIMPLE algorithm is used [37]. The interaction between chemistry and turbulence is modeled using the Probability Density Function (PDF) to solve a single transport equation [38]. The non-premixed combustion model in ANSYS Fluent includes a coal calculator function that requires entering proximate and ultimate analysis data from Table 1. This model uses a Probability Density Function (PDF) to represent the combustion products produced, which in this study is an analysis of the combustion products of oxy-fuel combustion, namely C, CO_2, H_20, and O_2. The solver settings include Discrete Ordinates (DO) for heat transfer and K-epsilon for turbulent models; the numerical steps of the methodology flow chart can be seen in Fig. 1.

Table 1. Kalimantan coals characteristics [35]

Proximate analysis	Coal
Volatile matter	43.28
Fixed carbon	38.16
Ash	6.78
Moisture	11.78
Ultimate analysis	
C	59.48
H	4.08
O	28.72
N	0.75
S	0.19
Air	
N_2	79
O_2	21

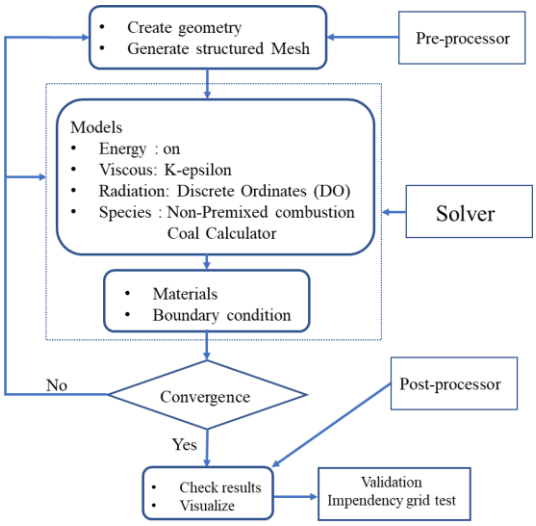

Fig. 1. CFD numerical methodology flow chart.

Heat transfer to the mixture on the walls of the combustion chamber is non-adiabatic during coal burning in the furnace. The air-fuel ratio is 1:7, by which the volume content of oxygen in the air will vary. 21 vol.% oxygen is assumed to be combustion coal in ambient air, OF25 is combustion coal with 25 vol.% oxygen, and OF35 is combustion coal with 35 vols.% oxygen. And for OF30, it is 30 vol.% O_2. The combustion chamber walls have isothermal limit conditions determined by the control volume walls remaining at a constant temperature of 1200 ºC on the wall in the CFD domain. Because of the symmetry, only half of the feeder and furnace chambers are simulated. The center line for the domain details in Fig. 2 is where the axes of symmetry are utilized.

Fig. 3 is the structured mesh used in this study. Before simulating the variation of oxygen concentration, in Fig. 4, an independent mesh is first performed to measure the accuracy of the simulation based on the number of grids structured with the result of mass fraction of CO_2 in the center axis DTF. The first grid is 5,036 nodes, the second is 102,051 nodes, the third is 150,772 nodes, the fourth is 200,078 nodes, and the fifth is 257,823 nodes. The second grid is multiple times the first until the fifth grid. It is then tested to ensure that the grid amount did not affect the results. Then the third grid for the simulation of oxygen concentration variations.

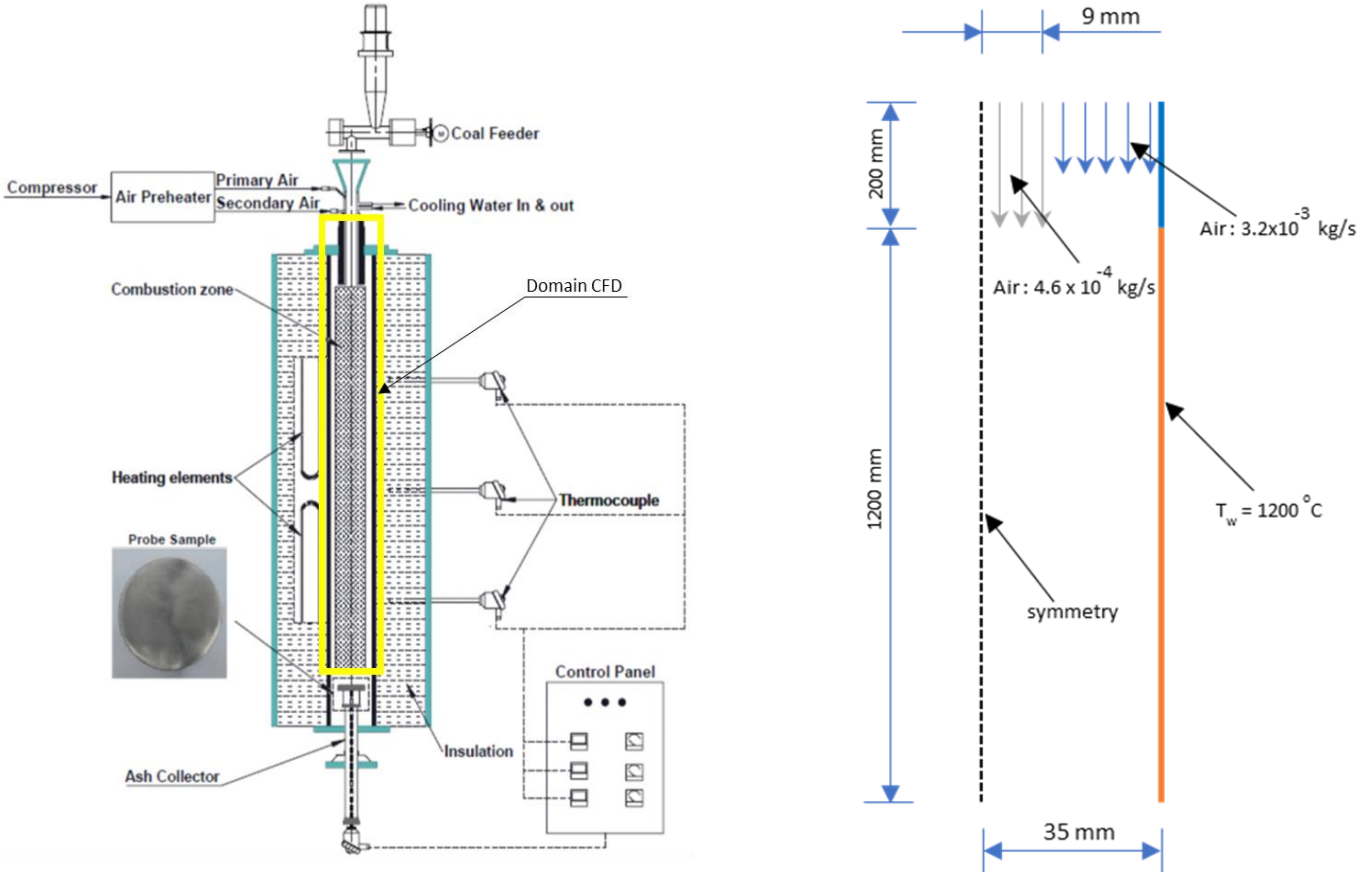

Fig. 2. DTF schematic diagram DTF [35] and CFD domain.

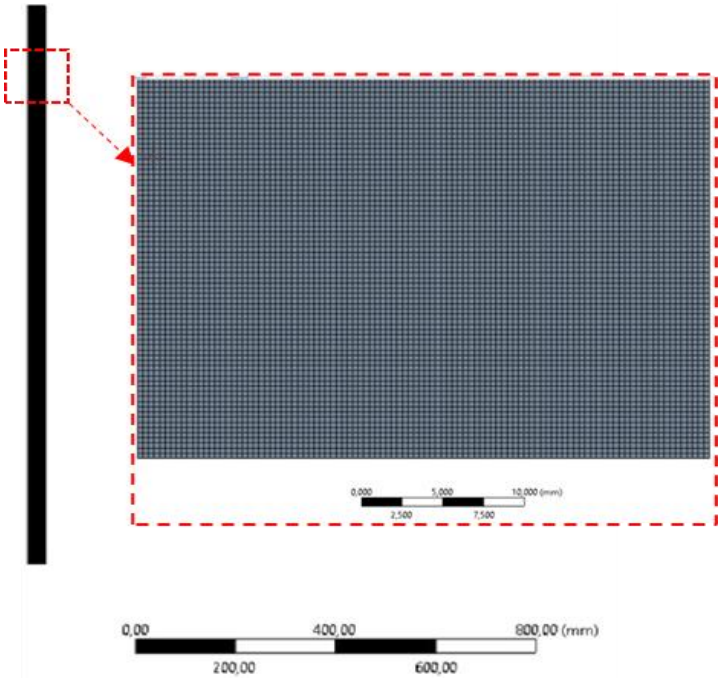

Fig. 3. Structured grid.

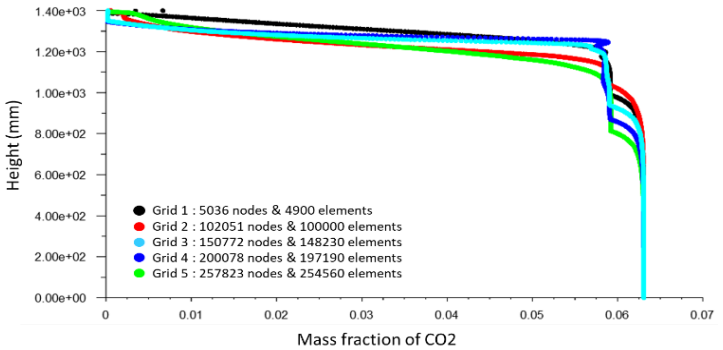

Fig. 4. Grid independence tests of mass fraction of CO_2 in various grids.

4 Results and Discussion

The numerical study of oxy-fuel combustion in a 2-D symmetry DTF was investigated. Fig. 5 illustrates the combustion temperature of coal in the center line of DTF when used with ambient air, assuming 21 vol.% O_2, 25 vol.% O_2, and 30 vol.% O_2. The figure indicates that combustion occurs at the beginning of entering the header, where the coal (21% O_2) temperature is lower than OF25 and OF30. Combustion starts in the header at OF25 and OF30, but for coal, it occurs after the header. This suggests that the higher the oxygen volume, the higher the temperature, but with a shorter flame distance. As the DTF furnace operates at 1200 ºC, the combustion temperature for high oxygen levels remains stable, which is visible in OF25 and OF30. The higher oxygen concentration allows for more efficient combustion and enhanced heat transfer, leading to higher flame temperatures [39]–[42]. Oxy-fuel combustion products are potent radiative gases, meaning they emit and absorb thermal radiation more efficiently. The increased concentration of radiative gases enhances the heat transfer within the combustion system, leading to higher temperatures [43] [44] (Fig. 6).

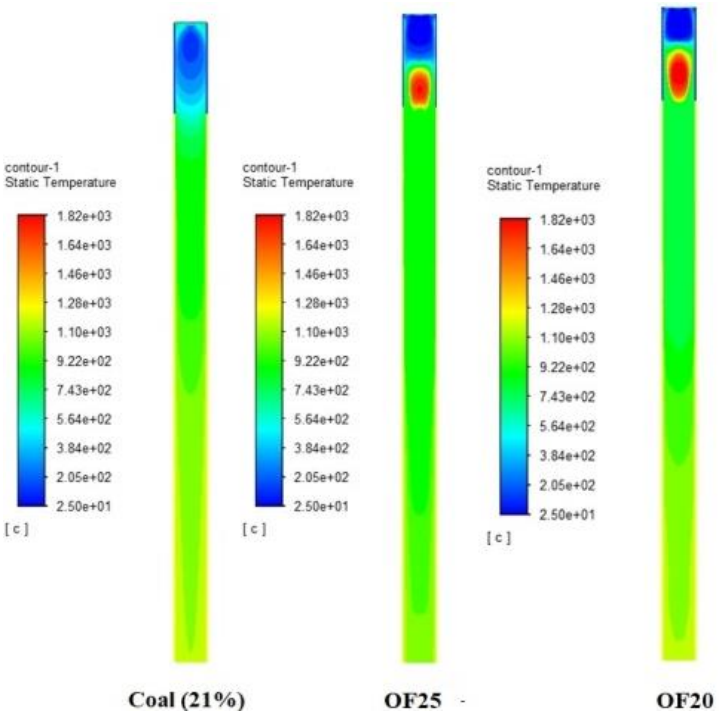

Fig. 6. The increased concentration of radiative gases.

Fig. 7 illustrates the variation in the mass fraction of O_2 during coal combustion for OF25 and OF30. In the top (inlet), it can be seen that the mass fraction of O_2 is still high and then drops due to the combustion process. When combusting coal with a volume fraction of 21% oxygen, it can be seen that oxygen is used up in combustion at a height of 1000 mm. However, in OF25, with a volume fraction of 25% oxygen, oxygen remains at a mass fraction of 0.01. The difference is even more significant in OF30 with a volume fraction of 30%, where the mass fraction of O_2 is 0.06. Increasing the oxygen concentration can improve the combustion process and efficiency in oxy-fuel combustion. However, even with higher oxygen concentrations, residual oxygen can still be present for several reasons.

First, combustion reactions require a specific ratio of fuel to oxygen for complete combustion. This ratio is known as the stoichiometric ratio. If the oxygen concentration exceeds this ratio, it can result in excess oxygen remaining after combustion [45]. Achieving the perfect mixing of fuel and oxygen is challenging in practical combustion systems. Incomplete mixing can lead to areas with fuel-rich or fuel-lean conditions, where some oxygen may not come into contact with the fuel to support complete combustion [46].

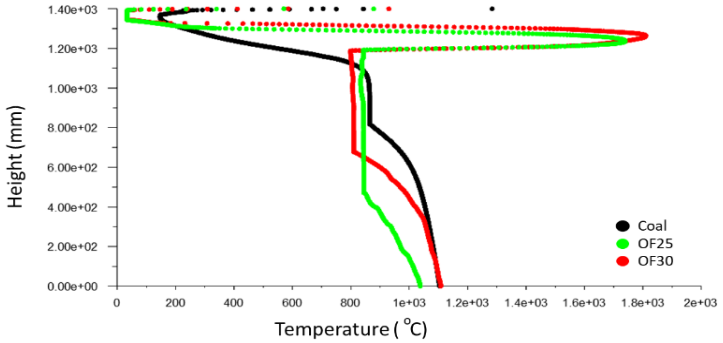

Fig. 5. Contour and graph of comparison temperature.

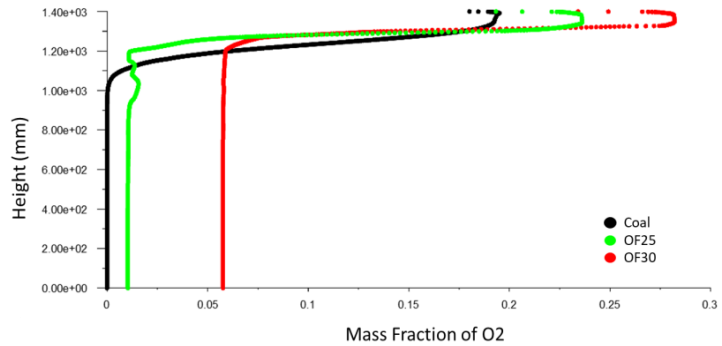

Fig. 7. Graph of comparison O_2.

The duration of time that the fuel and oxygen spend in the combustion zone also affects the combustion process. If the residence time is insufficient, complete combustion may not occur, and some oxygen may remain unreacted [47]. Using pure oxygen or oxygen-enriched air makes the oxygen concentration in the combustion process significantly higher than regular air combustion. This results in a higher combustion temperature, promoting more complete fuel oxidation and the generation of additional water vapor as a by-product [48]. Also, The participation of H_2O in the combustion atmosphere increased carbon conversion [49]. Fig. 8 explains the formation of H_2O during combustion, and higher oxygen make increases the mass fraction of H_2O. The mass fraction of H_2O in OF25 and OF30 is more significant than in coal.

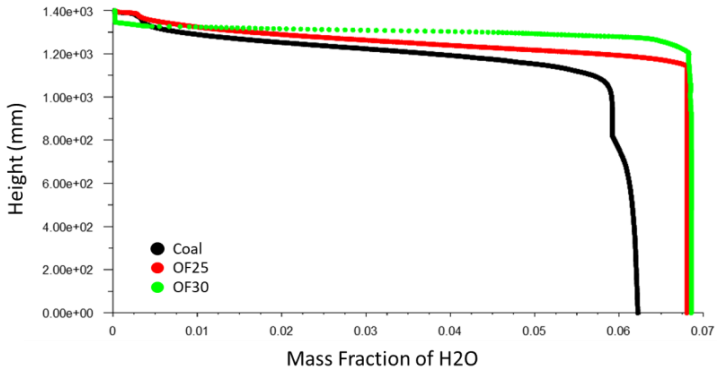

Fig. 8. Graph of comparison H_2O.

Fig. 9 explains the difference in the mass fraction of carbon, where the higher the oxygen volume fraction, the faster carbon is burnt. Increased oxygen concentration provides a more oxygen-rich environment, enhancing the combustion process and accelerating the reaction rate. In oxy-fuel combustion, nitrogen is mainly eliminated since oxygen is supplied separately. As a result, the absence of nitrogen allows for higher oxygen availability and promotes faster carbon combustion [50], [51]. However, this study cannot compare char mass fraction because the combustion equation with the Probability Density Function (PDF) does not accommodate the transformation of solid particles into char.

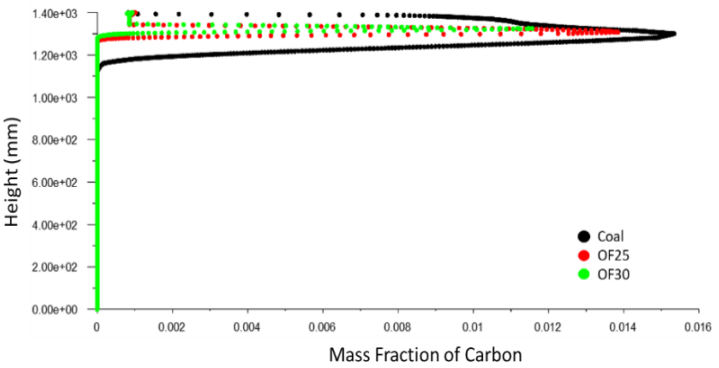

Fig. 9. Graph of comparison C.

Furthermore, CO_2 concentrations are very high during oxy-fuel combustion [52]. Fig. 10 shows that increasing the volume fraction of O_2 increases the mass fraction of CO_2. The gap between coal and OF25 is quite large, but between OF25 and OF30 is small.

5 Conclusions

To study the differences in combustion temperature and levels of O_2, H_2O, carbon, and CO_2, three types of combustion (coal, OF25, OF30) were simulated using a drop tube furnace and pulverized Kalimantan coal. Fluent, a commercial software for Computational Fluid Dynamics (CFD), was employed to simulate and examine the entirety of the combustion process. By adjusting the amount of oxygen in the inlet, the oxy-fuel combustion cases were able to meet the necessary conditions for combustion. However, using the Probability Density Function (PDF) model cannot describe the change in fuel particles to char. The results obtained from the numerical analysis indicated slight differences between the combustion temperature distribution and O_2 concentration in the oxy-fuel (OF25) combustion case and the coal case. However, these differences increased with higher levels of OF30. The flame structure was also shorter on the side inlet header due to higher oxygen consumption. Furthermore, the mass fraction of CO_2 in the oxy-fuel combustion environments was observed to have increased.

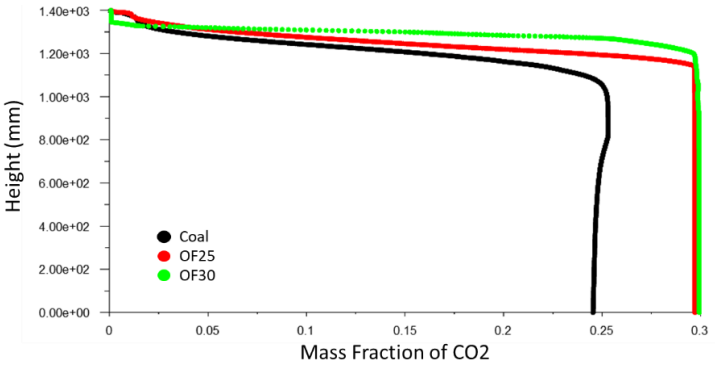

Fig. 10. Graph of comparison CO_2.

References

[1] T. Wall *et al.*, "An overview on oxy-fuel coal combustion—State of the art research and technology development," *Chem. Eng. Res. Des.*, vol. 87, no. 8, pp. 1003–1016, 2009, doi: https://doi.org/10.1016/j.cherd.2009.02.005.

[2] J. Davison, "Performance and costs of power plants with capture and storage of CO2," *Energy*, vol. 32, no. 7, pp. 1163–1176, 2007, doi: https://doi.org/10.1016/j.energy.2006.07.039.

[3] M. Kanniche, R. Gros-Bonnivard, P. Jaud, J. Valle-Marcos, J.-M. Amann, and C. Bouallou, "Pre-combustion, post-combustion and oxy-combustion in thermal power plant for CO2 capture," *Appl. Therm. Eng.*, vol. 30, no. 1, pp. 53–62, 2010, doi: https://doi.org/10.1016/j.applthermaleng.2009.05.005.

[4] M. Hanifa, R. Agarwal, U. Sharma, P. C. Thapliyal, and L. P. Singh, "A review on CO2 capture and sequestration in the construction industry: Emerging approaches and commercialized technologies," *J. CO2 Util.*, vol. 67, p. 102292, 2023, doi: https://doi.org/10.1016/j.jcou.2022.102292.

[5] B. J. P. Buhre, L. K. Elliott, C. D. Sheng, R. P. Gupta, and T. F. Wall, "Oxy-fuel combustion technology for coal-fired power generation," *Prog. Energy Combust. Sci.*, vol. 31, no. 4, pp. 283–307, 2005, doi: https://doi.org/10.1016/j.pecs.2005.07.001.

[6] E. J. Anthony and R. T. Symonds, "Oxy-fuel Firing Technology for Power Generation and Heat and Steam Production," in *Handbook of Climate Change Mitigation and Adaptation*, M. Lackner, B. Sajjadi, and W.-Y. Chen, Eds. New York, NY: Springer New York, 2020, pp. 1–27. doi 10.1007/978-1-4614-6431-0_39-3.

[7] ADB, *Carbon Dioxide-Enhanced Oil Recovery in Indonesia:* no. December. 2019. [Online]. Available: https://www.adb.org/publications/carbon-dioxide-enhanced-oil-recovery-indonesia

[8] A. A. Bhuiyan and J. Naser, "Numerical modeling of oxy-fuel combustion, the effect of radiative and convective heat

transfer and burnout," *Fuel*, vol. 139, pp. 268–284, 2015, doi: https://doi.org/10.1016/j.fuel.2014.08.034.
[9] L. Álvarez *et al.*, "CFD modeling of oxy-coal combustion in an entrained flow reactor," *Fuel Process. Technol.*, vol. 92, no. 8, pp. 1489–1497, 2011, doi: https://doi.org/10.1016/j.fuproc.2011.03.010.
[10] L. Álvarez *et al.*, "CFD modeling of oxy-coal combustion: Prediction of burnout, volatile and NO precursors release," *Appl. Energy*, vol. 104, pp. 653–665, 2013, doi: https://doi.org/10.1016/j.apenergy.2012.11.058.
[11] J. Zhang, W. Prationo, L. Zhang, and Z. Zhang, "Computational Fluid Dynamics Modeling on the Air-Firing and Oxy-fuel Combustion of Dried Victorian Brown Coal," *Energy & Fuels*, vol. 27, no. 8, pp. 4258–4269, Aug. 2013, doi: 10.1021/ef400032t.
[12] J. Zhang *et al.*, "Pilot-scale experimental and CFD modeling investigations of oxy-fuel combustion of Victorian brown coal," *Fuel*, vol. 144, pp. 111–120, 2015, doi: https://doi.org/10.1016/j.fuel.2014.12.026.
[13] R. D. Jovanović, K. Strug, B. Swiatkowski, S. Kakietek, K. Jagiello, and D. B. Cvetinović, "Experimental and numerical investigation of flame characteristics during swirl burner operation under conventional and oxy-fuel conditions," *Therm. Sci.*, vol. 21, no. 3, pp. 1463–1477, 2017, doi: 10.2298/TSCI161110325J.
[14] Z. Ying, C. Lixin, L. Qiao, C. Guozan, and Y. Xuchu, "Simulating the Process of Oxy-Fuel Combustion in the Sintering Zone of a Rotary Kiln to Predict Temperature, Burnout, Flame Parameters and the Yield of Nitrogen Oxides," *Chem. Technol. Fuels Oils*, vol. 54, no. 5, pp. 650–660, 2018, doi: 10.1007/s10553-018-0971-2.
[15] Z. F. Abdul Gani and P. Arun Pandian, "Modelling of coal combustion in a drop tube furnace in air and oxy-fuel environment," *Mater. Today Proc.*, vol. 47, pp. 4431–4437, 2021, doi: https://doi.org/10.1016/j.matpr.2021.05.269.
[16] D. T. Pratt, L. Smoot, and D. Pratt, *Pulverized coal combustion and gasification*. Springer, 1979. doi https://doi.org/10.1007/978-1-4757-1696-2.
[17] V. Sahajwalla, A. Eghlimi, and K. Farrell, "Numerical simulation of pulverized coal combustion," *CSIRO Div. Miner. Melbourne, Vic.*, 1997, [Online]. Available: https://www.osti.gov/etdeweb/biblio/300871
[18] M. Sijercic, S. Belosevic, and P. Stefanovic, "Modeling of pulverized coal combustion stabilization by means of plasma torches," *Therm. Sci.*, vol. 9, no. 2, pp. 57–72, 2005, doi: 10.2298/tsci0502057s.
[19] P. Madejski, "Numerical study of a large-scale pulverized coal-fired boiler operation using CFD modeling based on the probability density function method," *Appl. Therm. Eng.*, vol. 145, pp. 352–363, 2018, doi: https://doi.org/10.1016/j.applthermaleng.2018.09.004.
[20] M. Stöllinger, B. Naud, D. Roekaerts, N. Beishuizen, and S. Heinz, "PDF modeling and simulations of pulverized coal combustion – Part 2: Application," *Combust. Flame*, vol. 160, no. 2, pp. 396–410, 2013, doi: https://doi.org/10.1016/j.combustflame.2012.10.011.
[21] J. Zheng, B. Liu, and B. Liu, "Simulation of Pulverized Coal Combustion Process Considering Turbulence-Radiation Interaction," *ACS Omega*, 2023, doi: 10.1021/acsomega.3c00115.
[22] B. Zhu, B. Shang, X. Guo, C. Wu, X. Chen, and L. Zhao, "Study on Combustion Characteristics and NOx Formation in 600 MW Coal-Fired Boiler Based on Numerical Simulation," *Energies*, vol. 16, no. 1, 2023, doi: 10.3390/en16010262.
[23] J. Zheng, B. Liu, and B. Liu, "Simulation of Pulverized Coal Combustion Process Considering Turbulence–Radiation Interaction," *ACS Omega*, vol. 8, no. 14, pp. 12944–12954, Apr. 2023, doi: 10.1021/acsomega.3c00115.
[24] M. Rieth, A. G. Clements, M. Rabaçal, F. Proch, O. T. Stein, and A. M. Kempf, "Flamelet LES modeling of coal combustion with detailed devolatilization by directly coupled CPD," *Proc. Combust. Inst.*, vol. 36, no. 2, pp. 2181–2189, 2017, doi: https://doi.org/10.1016/j.proci.2016.06.077.
[25] W. Sun, W. Zhong, and T. Echekki, "Large eddy simulation of non-premixed pulverized coal combustion in corner-fired furnace for various excess air ratios," *Appl. Math. Model.*, vol. 74, pp. 694–707, 2019, doi: https://doi.org/10.1016/j.apm.2019.05.017.
[26] Y. Yang *et al.*, "Investigation on the effects of different forms of sodium, chlorine and sulfur and various pretreatment methods on the deposition characteristics of Na species during pyrolysis of a Na-rich coal," *Fuel*, vol. 234, pp. 872–885, 2018, doi: https://doi.org/10.1016/j.fuel.2018.07.130.
[27] X. Li, X. Gong, C. Zhang, T. Liu, W. Wang, and Y. Zhang, "Occurrence characteristics of ash-forming elements in sea rice waste and their effects on particulate matter emission during combustion," *Fuel*, vol. 273, p. 117769, 2020, doi: https://doi.org/10.1016/j.fuel.2020.117769.
[28] S. Hui, Y. Lv, Y. Niu, S. Li, Y. Lei, and P. Li, "Effects of leaching and additives on the formation of deposits on the heating surface during high-Na/Ca Zhundong coal combustion," *J. Energy Inst.*, vol. 94, pp. 319–328, 2021, doi: https://doi.org/10.1016/j.joei.2020.09.016.
[29] J. Han *et al.*, "Fine Ash Formation and Slagging Deposition during Combustion of Silicon-Rich Biomasses and Their Blends with a Low-Rank Coal," *Energy \& Fuels*, vol. 33, no. 7, pp. 5875–5882, 2019, doi: 10.1021/acs.energyfuels.8b04193.
[30] B. Yan, Y. Cheng, Y. Jin, and C. Y. Guo, "Analysis of particle heating and devolatilization during rapid coal pyrolysis in a thermal plasma reactor," *Fuel Process. Technol.*, vol. 100, pp. 1–10, 2012, doi: https://doi.org/10.1016/j.fuproc.2012.02.009.
[31] M. R. Safaei, H. Goshayeshi, B. Razavi, and M. Goodarzi, "Numerical investigation of laminar and turbulent mixed convection in a shallow water-filled enclosure by various turbulence methods," vol. 6, 2010, [Online]. Available: https://www.researchgate.net/publication/267850752_Numerical_investigation_of_laminar_and_turbulent_mixed_convection_in_a_shallow_water-filled_enclosure_by_various_turbulence_methods
[32] Z. Q. Li, F. Wei, and Y. Jin, "Numerical simulation of pulverized coal combustion and NO formation," *Chem. Eng. Sci.*, vol. 58, no. 23, pp. 5161–5171, 2003, doi: https://doi.org/10.1016/j.ces.2003.08.012.
[33] M. Goodarzi *et al.*, "Numerical Study of Entropy Generation due to Coupled Laminar and Turbulent Mixed Convection and Thermal Radiation in an Enclosure Filled with a Semitransparent Medium," *Sci. World J.*, vol. 2014, p. 761745, 2014, doi: 10.1155/2014/761745.
[34] S. Parker, D. Kahrimanovic, and C. Goniva, "Improving the applicability of discrete phase simulations by smoothening their exchange fields," *Appl. Math. Model.*, vol. 35, no. 5, pp. 2479–2488, 2011, doi: https://doi.org/10.1016/j.apm.2010.11.066.
[35] Hariana, F. Karuana, Prabowo, E. Hilmawan, A. Darmawan, and M. Aziz, "Effects of Different Coals for Co-Combustion with Palm Oil Waste on Slagging and Fouling Aspects," *Combust. Sci. Technol.*, vol. 00, no. 00, pp. 1–23, 2022, doi: 10.1080/00102202.2022.2152684.
[36] M. R. Safaei, B. Rahmanian, and M. Goodarzi, "Numerical study of laminar mixed convection heat transfer of power-

law non-Newtonian fluids in square enclosures by finite volume method," vol. 6, 2010, doi: 10.5897/ijps11.1092.
[37] M. Goodarzi *et al.*, "Investigation of nanofluid mixed convection in a shallow cavity using a two-phase mixture model," *Int. J. Therm. Sci.*, vol. 75, pp. 204–220, 2014, doi: https://doi.org/10.1016/j.ijthermalsci.2013.08.003.
[38] B. Rahmanian, M. R. Safaei, S. N. Kazi, G. Ahmadi, H. F. Oztop, and K. Vafai, "Investigation of pollutant reduction by simulation of turbulent non-premixed pulverized coal combustion," *Appl. Therm. Eng.*, vol. 73, no. 1, pp. 1222–1235, 2014, doi: 10.1016/j.applthermaleng.2014.09.016.
[39] Y. Kuang, B. He, W. Tong, C. Wang, and Z. Ying, "Effects of oxygen concentration and inlet velocity on pulverized coal MILD combustion," *Energy*, vol. 198, p. 117376, 2020, doi: https://doi.org/10.1016/j.energy.2020.117376.
[40] A. Mittal, A. Saxena, and B. Mohapatra, "Oxygen Enrichment Technology---An Innovation for Improved Solid Fuel Combustion and Sustainable Environment," in *Enhancing Future Skills and Entrepreneurship*, 2020, pp. 13–19.
[41] K.-K. Wu, Y.-C. Chang, C.-H. Chen, and Y.-D. Chen, "High-efficiency combustion of natural gas with 21–30% oxygen-enriched air," *Fuel*, vol. 89, no. 9, pp. 2455–2462, 2010, doi: https://doi.org/10.1016/j.fuel.2010.02.002.
[42] S. SadatAkhavi, S. Tabejamaat, M. EiddiAttarZade, and B. Kankashvar, "Experimental and numerical study of combustion characteristics in a liquid fuel CAN micro-combustor," *Aerosp. Sci. Technol.*, vol. 105, p. 106023, 2020, doi: https://doi.org/10.1016/j.ast.2020.106023.
[43] W. Nimmo, S. S. Daood, and B. M. Gibbs, "The effect of O2 enrichment on NOx formation in biomass co-fired pulverized coal combustion," *Fuel*, vol. 89, no. 10, pp. 2945–2952, 2010, doi: https://doi.org/10.1016/j.fuel.2009.12.004.
[44] Z. Zhou, Q. Xue, C. Li, G. Wang, X. She, and J. Wang, "Coal flow and combustion characteristics under oxygen enrichment way of oxygen-coal double lance," *Appl. Therm. Eng.*, vol. 123, pp. 1096–1105, 2017, doi: https://doi.org/10.1016/j.applthermaleng.2017.05.177.
[45] S.-S. Hou, C.-Y. Chiang, and T.-H. Lin, "Oxy-Fuel Combustion Characteristics of Pulverized Coal under O2/Recirculated Flue Gas Atmospheres," *Appl. Sci.*, vol. 10, no. 4, 2020, doi: 10.3390/app10041362.
[46] P. Baskar and A. Senthilkumar, "Effects of oxygen-enriched combustion on pollution and performance characteristics of a diesel engine," *Eng. Sci. Technol. an Int. J.*, vol. 19, no. 1, pp. 438–443, 2016, doi: https://doi.org/10.1016/j.jestch.2015.08.011.
[47] Y. Xu, Y. Bu, M. Chen, M. Yu, and L. Wang, "Characteristics for Oxygen-Lean Combustion and Residual Thermodynamics in Coalfield-Fire Zones within Axial Pressure.," *ACS Omega*, vol. 5, no. 35, pp. 22502–22512, Sep. 2020, doi: 10.1021/acsomega.0c03108.
[48] H. Christoph and S. S. Kuldip, *Enhancing Future Skills and Entrepreneurship*, vol. 49, no. 0. 2020.
[49] C. Bu, A. Gómez-Barea, B. Leckner, X. Wang, J. Zhang, and G. Piao, "The effect of H2O on the oxy-fuel combustion of a bituminous coal char particle in a fluidized bed: Experiment and modeling," *Combust. Flame*, vol. 218, pp. 42–56, 2020, doi: 10.1016/j.combustflame.2020.03.025.
[50] S. Yadav and S. S. Mondal, "A review on the progress and prospects of oxy-fuel carbon capture and sequestration (CCS) technology," *Fuel*, vol. 308, p. 122057, 2022, doi: https://doi.org/10.1016/j.fuel.2021.122057.
[51] M. B. Toftegaard, J. Brix, P. A. Jensen, P. Glarborg, and A. D. Jensen, "Oxy-fuel combustion of solid fuels," *Prog. Energy Combust. Sci.*, vol. 36, no. 5, pp. 581–625, 2010, doi: https://doi.org/10.1016/j.pecs.2010.02.001.
[52] J. M. Beér *et al.*, "Oxy-Fuel Combustion for Power Generation and Carbon Dioxide (CO2) Capture," in *Woodhead Publishing*, L. Zheng, Ed. Woodhead Publishing, 2011, pp. xi–xiii. doi https://doi.org/10.1016/B978-1-84569-671-9.50018-1.